Program Digest, 2019 IEEE International Ultrasonics Symposium (IUS)
Glasgow, Scotland, October 6-9, 2019

Nonlinear acoustic characterization of the shell and size engineered microbubbles and nanobubbles

NR Shirazi [1,2,3],AJ Sojahrood [1,2,3],H Haghi [1,2,3], G fishbein [1,2,3], A de Leon [4], A Exner [4] & MC Kolios [1,2,3]
[1] *Department of Physics, Ryerson University, Toronto, Ontario, Canada*
[2] *Institute for Biomedical Engineering Science and Technology, St. Michael's Hospital, Toronto, Ontario,Canada*
[3] *Keenan Research Centre for Biomedical Science, Toronto, Ontario, Canada*
[4] *Department of Radiology, Case Western Reserve University, Cleveland, U.S.*

Abstract*—Optimization of the bubble performance requires size isolation and accurate shell characterization using models that are not limited by linear assumptions. MBs and NBs with 2 different shell compositions (crosslinked (C) and non-crosslinked (NC)) were made in-house. NC shell is made with 4 different lipids including DBPC, DPPA,DPPE and DSPE-PEG2000 . C shell bubbles have additional ingredients that produce a UV polymerized crosslinked shell. Using the method of multiple differential centrifugations, two distinct size populations were separated with mean diameters of 2.9 μm for NC-MB and 3.3 μm for C-MB. The attenuation and sound speed of the diluted solutions were measured through transmission and reception method using one pair of PVDF transducers with center frequencies of 10 MHz and 100$\%$ BW at acoustic pressures of approximately 5 to 40 kPa. Our nonlinear model accounting for large amplitude MB oscillations was used to fit the measured attenuation and sound speed data at each pressure. As the pressure increased from 5 kPa to $\approx 50kPa$, resonance frequency (f_r) of the NC-MBs with a mean diameter (MD) of 2.9 μm decreased from 9.1 to 5.9 MHz and f_r of the C-MBs with (MD) of 3.3 μm decreased from 8 to 4.8 MHz. NC-NB solutions did not display any attenuation peak in the frequency range of 2-10 MHz, additionally; the measured attenuation was 5-10 times smaller than the MBs with the same shell composition. Fitting of the shell parameters suggests that crosslinking the shell results in $\approx$ 37$\%$ increase in stiffness and 50 $\%$ decrease in shell viscosity. The lower attenuation of the NBs even at very high concentrations may explain the enhancement in NB contrast ultrasound.

I. Introduction

The outcome of the therapeutic and diagnostic applications of microbubbles (MBs) and nanobubbles (NBs) depends on their nonlinear behavior. Nonlinear behavior of the MBs depends on their size, shell composition and on the applied acoustic pressure and frequency. Because of the polydispersity of bubbles in most applications, only subpopulations of the size distribution may be fully active. Characterization of bubble shell parameters is usually performed through attenuation measurements and fitting using linear or semi-linear models [1]–[6]. These models are not applicable at the higher pressures that are employed in most applications [7], [8]. Optimization of the bubble performance requires size isolation and accurate shell characterization using models that are not limited by linear assumptions [8].

It is numerically shown that the resonance frequency (f_r) and subharmponic resonance frequency of MBs (f_{sh}) of the MBs decreases with pressure increase [9]–[11]. The change in pressure dependent resonance frequency have been confirmed by many experimental observations of sonication of mono-disperse lipid coated bubbles [5], [8], [12], [13]. We have recently developed a model for predicting the pressure dependent attenuation and sound speed of the bubbly media [7], [8]. Predictions of the model were in good agreements with the experimental observations [8]. The advantage of the nonlinear model is that it is not limited to linear oscillations ranges and includes the nonlinear large amplitude oscillations. In this work effects of size and shell compositions are examined through broadband attenuation measurements of two MBs and NBs with 2 different shell compositions (crosslinked (C) and non-crosslinked (NC)) ate different excitation pressure amplitudes. The nonlinear model [7], [8] was then used to estimate the shell parameters of the MBs. Effect of pressure on the changes of the resonance frequency of the bubble solutions was studied.

II. Experiments

A. Bubble preparation

All glassware was washed and cleaned with 70$\%$ ethyl alcohol and then air dried. The gas used to form microbubbles and nanobubbles was octafluoropropane (C3F8). Lipid mixture of 60.1 mg of 1,2-dipalmitoyl-sn-glycero-3-phosphocholine (DBPC), 10 mg of 1,2-dipamitoyl-sn-glycero-3-phosphate, sodium salt (DPPA), 10 mg of 1,2 distearoyl-sn-glycero-3-phosphothanolamine-N-[amino (polyethylene glycol)-2000] (DSPE-mPEG) as well as 20 mg of 1,2-dipalmitoyl-sn-glycero-3-phosphothanolamine (DPPE) were added together in a glass vial. To prepare PGG (Propylene glycol- glycerol) bubbles, 1 mL Propylene glycol was added to the lipid mixture and heated at 80° water bath for 15 minutes and dissolve by sonicating every minute. A mixture of 8 mL of Phosphate Buffer Saline (PBS) and 1 mL of glycerol was heated at the same temperature and then added to the mixture of lipids and Propylene glycol. Finally, the mixture was sonicated for 10 minutes to obtain a homogeneous solution. 1 mL of the solution was transferred to a 3 mL vial and then cap and sealed. Before activation of the vial, the gas inside the vial was exchanged with C3F8 and then the vial was shaken for 45 seconds with a mechanical shaker (VialMix) [14]. To prepare the cross link (Xlink) microbubbles [15], same lipid mixture as PGG were prepared, additionally, a mixture of 34 μL of N,

978-1-7281-4595-2/19/$31.00 ©2019 IEEE

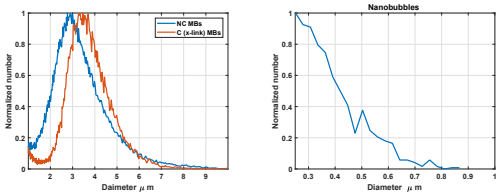

(a) (b)

Fig. 1. Normalized size distribution of a) NC and C MBs and b) NBs.

N-Diethylacrylamide (NNDA) and 5 mg of 2-Hydroxy-4'-(2-hydroxyethoxy)-2 methylpropiophenone (Irgacure) and 5 mg of N, N'-Bis(acryloyl) cystamine (BAC) were added to the glass vial as well. A mixture of 8 mL PBS and 1 mL of glycerol was heated at the same temperature and then added to the mixture of lipids and Propylene glycol. Finally, the mixture was sonicated for 10 minutes to obtain a homogeneous solution. 1 mL of the solution was transferred to a 3 mLvial and then cap and sealed. Before the activation of the vial, the gas inside the vial was exchanged with C3F8 and then shaken for 45 seconds with a mechanical shaker (ViialMix). The vial was opened, the small magnetic stir bar was added to the vial and then cap and sealed and the process of gas exchange was done again. Lastly, the mixture was polymerized with UV light at 257 nm for 30 minutes with continuous mixing at 54 RPM. For isolating nano-bubbles, After the activation of the bubbles, the vials were inverted and centrifuged at 50 RCF for 5 minutes and then drawn from the below the neck of the vial [14].

B. Microbubble isolation

After the activation, one vial containing native bubble population was collected into a 3mL syringe and the diluted into 100 mL filtered PBS. 30 mL syringes were used to draw the solution. Differential centrifugation technique [16] was used to isolate bubbles of different sizes. Syringes were centrifuged with 550 RPM (50 RCF) for 2 minutes in order to remove submicron bubbles. The white part resting against the plunger (cake) consisting microbubbles larger than 1 micron was re-diluted with 60 mL PBS and the infranatant consisting submicron bubbles was discarded. Next, syringes filled with re-diluted with 60 mL PBS and the cake was centrifuged with 960 RPM (160 RCF) for 2 minutes. The infranatant consisting less than 2 μm bubbles were discarded, and the cake was re-diluted again with 60 mL PBS. Finally, syringes were filled with the new solution and then centrifuged with 1040 RPM (180 RCF). The infranatant was discarded and the cake was re-dispersed with 20 mL PBS.

III. Numerical procedure

A. Nonlinear-Model

Starting with the Caflisch equation [17] for the propagation of the acoustic waves in a bubbly medium we have derived the pressure dependent equations for the imaginary and real part of the wave number suared in [7], [8]:

$$\langle \Re(k^2) \rangle = \frac{-\omega^2}{C_l^2} - \frac{2\rho_l}{T|P|^2} \sum_{i=1}^{N} \int_0^T \Re(P) \frac{\partial^2 \beta_i}{\partial t^2} dt \qquad (1)$$

$$\langle \Im(k^2) \rangle = -\frac{2\rho_l}{T|P|^2} \sum_{i=1}^{N} \int_0^T \Im(P) \frac{\partial^2 \beta_i}{\partial t^2} dt \qquad (2)$$

where $\Re$ and $\Im$ respectively denote the real and imaginary parts, k is the wave number,<> denotes the time average, P is pressure, C_l is the speed of sound in the liquid in the absence of bubbles, ρ_l is the liquid density, ω is the angular frequency of a propagating wave, T is the time averaging interval and β_i is the local volume fraction occupied by the gas at time t of the *ith* MBs. $\beta_i$is given by $\beta_i(t) = \frac{4}{3}\pi R_i(t)^3 N_i$ where R_i *(t)* is the instantaneous radius of the MBs with initial radius of R_{0i} and N_i is the number of the corresponding MBs per unit volume in the medium and summation is performed over the whole population of the MBs. k=k_r-$i\alpha$ and the sound speed can be calculated from k_r which is the real part of the wave number, and the attenuation α from the imaginary part of the wave number. contribution of each MBs with β_i is summed. Using Eqs. 1 and 2, we can now calculate the pressure-dependent sound speed and attenuation in a bubbly medium. To do this, the radial oscillations of the MBs in response to an acoustic wave were calculated first. Then equation 1 and 2 were solved by integrating over the β_i of each of the MBs in the population. The accuracy of the model was verified in [7], [8] compared to the results of linear models [6], semi-linear models [18] and experiments.

B. The bubble model

To numerically simulate the attenuation and sound speed, the Marmottant model [16], which accounts for radial-dependent shell properties (e.g. buckling and rupture), was modified to include MB multiple scattering using the approach introduced in [19]. The modified Marmottant model can be presented as:

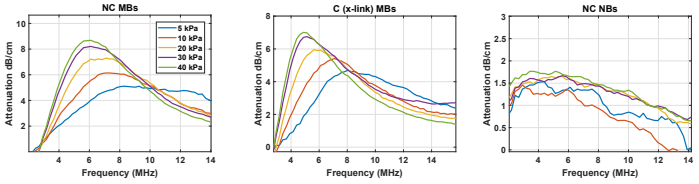

(a) (b) (c)

Fig. 2. Measured attenuation of the a) NC MBs (blue curve in fig. 1a) with $5.67 * 10^6 MBs/ml$, b)a) C MBs (red curve in fig. 1a) with $1.78 * 10^6 MBs/ml$ and c) NC NBs $\approx 8 * 10^{10} MBs/ml$.

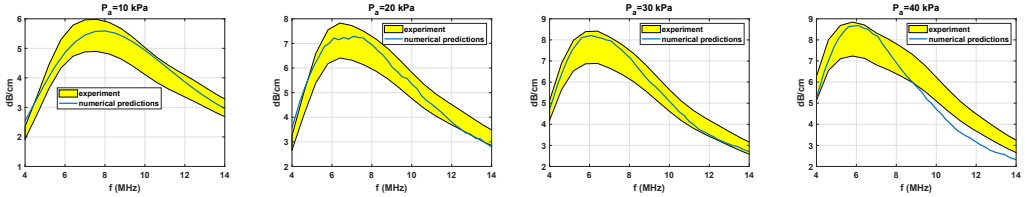

(a) (b) (c) (d)

Fig. 3. Numerical simulation (yellow) of the attenuation of the NC MBs (blue curve in fig. 1a) with $5.67 * 10^6 MBs/ml$.

$$R_i\ddot{R}_i + \frac{3}{2}\dot{R_i}^2 = \frac{1}{\rho}([P_0 + \frac{2\sigma(R_{0i})}{R_{0i}}](\frac{R_i}{R_{i0}})^{3k}(1 - \frac{3k}{C}\dot{R}_i) - \frac{2\sigma(R_i)}{R_i} - \frac{4\mu\dot{R}_i}{R_i} - \frac{4\kappa_s\dot{R}_i}{R_i^2} - P_{ac}(t)) - \sum_{j\neq i}\frac{R_j}{d_{ij}}(R_j\ddot{R}_j + 2\dot{R_j}^2), i = 1, .., N \quad (3)$$

In this equation R_{i0} is the initial radius of the ith bubble, P_0 is the atmospheric pressure C is the sound speed, k is the polytropic exponent, μ is the viscosity of the liquid. σ is the surface tension and is a function of bubble radius and is given by :

$$\sigma = \begin{cases} 0 & if \quad R <= R_b \\ \chi\left((\frac{R}{R_b})^2 - 1\right) & if \quad R_b < R < R_r \\ \sigma_{water} & if \quad R >= R_r \end{cases} \quad (4)$$

where σ_{water} is the water surface tension, R_b is the buckling radius, R_r is the rupture radius and χ is the shell elasticity. κ_s in equation 4, is the surface deiltational viscosity and is given by $\kappa_s = \frac{\kappa_{s0}}{1+\alpha\frac{|\dot{R}|}{R}}$ [20]. In this equation α is the characteristic time constant and in this study is $1 * 10^{-6}\mu s$.
Using the same appraoch as in [17], Equation 4 can be written in a Matrix format as:

$$\begin{pmatrix} \ddot{R}_1 \\ \ddot{R}_2 \\ ... \\ \ddot{R}_N \end{pmatrix} = \begin{pmatrix} R_1 & \frac{R_2^2}{d_{12}} & ... & \frac{R_N^2}{d_{1N}} \\ \frac{R_1^2}{d_{21}} & R_1 & ... & \frac{R_N^2}{d_{2N}} \\ ... & ... & ... & ... \\ \frac{R_1^2}{d_{N1}} & \frac{R_2^2}{d_{N2}} & ... & R_N \end{pmatrix}^{-1} \begin{pmatrix} A_1 \\ A_2 \\ ... \\ A_N \end{pmatrix} \quad (5)$$

where:

$$A_i = \frac{1}{\rho}\left(\left[P_0 + \frac{2\sigma(R_{0i})}{R_{0i}}\right]\left(\frac{R_i}{R_{i0}}\right)^{3k}\left(1 - \frac{3k}{C}\dot{R}_i\right) - \frac{2\sigma(R_i)}{R_i} - \frac{4\mu\dot{R}_i}{R_i} - \frac{4\kappa\dot{R}_i}{R_i^2} - P_{ac}(t) - \frac{3\rho}{2}\dot{R}_i^2\right) - \sum_{j\neq i}\frac{2R_j\dot{R}_j^2}{d_{ij}} \quad (6)$$

At each frequency and pressure, 100 MBs were selected from the size distribution measured during the experiments. Then they were randomly distributed in a cube with sides of d in length to simulate the concentration of bubbles in experiments. Thermal effects were not included in the simulations. We have shown on [22] that in case of coated bubbles that enclose gases similar to C3F8 thermal effects can be neglected.

IV. Results

A. Experiments

Figure 2 shows the measured attenuation of the NC MBs (blue curve in fig. 1a) with $5.67 * 10^6 MBs/ml$, C MBs (red curve in fig. 1a) with $1.78 * 10^6 MBs/ml$ and NC NBs ($\approx 5.6 * 10^{11} MBs/ml$). The frequency of the attenuation peak of the Nc MBs (mean diameter (MD)=2.9 μm) decreases from 9.1 MHz at $\approx 5kPa$ to 5.94 MHz at $\approx$ 40 kPa, and

Fitted shell parameters				
Shell type	$\chi\ (\frac{N}{m})$	$\sigma_0 \frac{N}{m}$	$\kappa_s\ \frac{kg}{s}$	$\alpha\ \mu s$
NC MBs	3.1±0.4	0.03 ± 0.05	(5.5±0.8)*10^{-8}	0.75±0.25
C MBs	5 ± 0.5	0.025 ± 0.07	(2.7±0.4)*10^{-8}	0.75±0.25

TABLE I
FITTED SHELL PARAMETERS.

the attenuation increases from 5.1 to 8.7 dB/cm (Fig. 2a). The frequency of the attenuation peak of the C MBs (mean diameter (MD)=3.3 μm) decrease from $\approx$ 8 MHz at $\approx 5kPa$ to $\approx$ 4.8 MHz and the attenuation increases from 4.7 to 7 dB/cm. NB solution does not have any observable peak and the maximum attenuation is $\approx 1.2-1.7dB/cm$ (Fig. 2b). Despite the small difference between the mean radii of the C and the NC MBs ($\approx 0.2mum$), the frequency of the attenuation peaks are distinctly different (e.g. 1.1 MHz at 5 kPa). Moreover, C bubbles have comparable attenuation to NC bubbles (e.g. 0.3 dB/cm difference at 100 kPa). This is , despite having a $\approx$ 3 times lower concentration than NC bubbles. This suggest that the cross linking of the shell significantly changes the shell parameters.

Figure 3 shows the results of the simulations for the NC MBs as a sample. The yellow curve is obtained by fitting the shell parameters to the experimental blue curve at different pressures. The estimated shell parameters of the C and NC bubbles are listed in Table 1. The average Shell elasticity for NC MBs at 4 different pressures was found to be 3.1 (N/m) and for the C MBs it was 5 (N/m). The average shell viscosity for NC MBs was estimated to be 5.5e-8 kg/s and for C MBs it was calculated to be 2.7e-8 kg/s. This suggests that the cross linking of the MBs shell, may modify the physical properties of the shell by increasing the shell elasticity and decreasing the shell viscosity.

V. DISCUSSION AND CONCLUSION

The estimated shell parameters suggest that crosslinking of the shell of the MBs can result in 37% increase in stiffness and 50% decrease in shell viscosity. This results was expected since the mixture of NNDEA and N,N-bis(acryoyl) cystamine (BAC) develops an interpenetrating cross linked network which enhance the stability [15] as well as the stiffness of the C MBs compare to NC MBs. The lower shell viscosity for the NC MBs may be due to less Glycerol content of the shell.

REFERENCES

[1] G. Eason, Goertz, D.E., de Jong, N. and van der Steen, A.F., 2007. Attenuation and size distribution measurements of Definity and manipulated Definity populations. Ultrasound in medicine & biology, 33(9), pp.1376-1388.

[2] Xia, L., Porter, T.M. and Sarkar, K., 2015. Interpreting attenuation at different excitation amplitudes to estimate strain-dependent interfacial rheological properties of lipid-coated monodisperse microbubbles. The Journal of the Acoustical Society of America, 138(6), pp.3994-4003.

[3] Shekhar, H., Smith, N.J., Raymond, J.L. and Holland, C.K., 2018. Effect of temperature on the size distribution, shell properties, and stability of Definity®. Ultrasound in medicine & biology, 44(2), pp.434-446.

[4] Helfield, B.L., Leung, B.Y., Huo, X. and Goertz, D.E., 2014. Scaling of the viscoelastic shell properties of phospholipid encapsulated microbubbles with ultrasound frequency. Ultrasonics, 54(6), pp.1419-1424.

[5] Segers, T., de Jong, N. and Versluis, M., 2016. Uniform scattering and attenuation of acoustically sorted ultrasound contrast agents: Modeling and experiments. The Journal of the Acoustical Society of America, 140(4), pp.2506-2517.

[6] Commander, K.W. and Prosperetti, A., 1989. Linear pressure waves in bubbly liquids: Comparison between theory and experiments. The Journal of the Acoustical Society of America, 85(2), pp.732-746.

[7] Sojahrood, A.J., Haghi, H., Karshafian, R. and Kolios, M.C., 2015, October. Nonlinear model of acoustical attenuation and speed of sound in a bubbly medium. In 2015 IEEE International Ultrasonics Symposium (IUS) (pp. 1-4). IEEE.

[8] Sojahrood, A.J., Li, Q., Haghi, H., Karshafian, R., Porter, T.M. and Kolios, M.C., 2018. Pressure dependence of the ultrasound attenuation and speed in bubbly media: Theory and experiment. arXiv preprint arXiv:1811.07788.

[9] Doinikov, A.A., Haac, J.F. and Dayton, P.A., 2009. Resonance frequencies of lipid-shelled microbubbles in the regime of nonlinear oscillations. Ultrasonics, 49(2), pp.263-268.

[10] Sojahrood, A.J., Falou, O., Earl, R., Karshafian, R. and Kolios, M.C., 2015. Influence of the pressure-dependent resonance frequency on the bifurcation structure and backscattered pressure of ultrasound contrast agents: a numerical investigation. Nonlinear Dynamics, 80(1-2), pp.889-904.

[11] Sojahrood, A.J., Earl, R., Li, Q., Porter, T.M., Kolios, M.C. and Karshafian, R., 2019. Nonlinear dynamics of acoustic bubbles excited by their pressure dependent subharmonic resonance frequency: oversaturation and enhancement of the subharmonic signal. arXiv preprint arXiv:1909.05071.

[12] Overvelde, M., Garbin, V., Sijl, J., Dollet, B., De Jong, N., Lohse, D. and Versluis, M., 2010. Nonlinear shell behavior of phospholipid-coated microbubbles. Ultrasound in medicine & biology, 36(12), pp.2080-2092.

[13] Gong, Y., Cabodi, M. and Porter, T.M., 2014. Acoustic investigation of pressure-dependent resonance and shell elasticity of lipid-coated monodisperse microbubbles. Applied Physics Letters, 104(7), p.074103.

[14] Perera, R., Hernandez, C., Cooley, M., Jung, O., Jeganathan, S., Abenojar, E., Fishbein, G., Sojahrood, A.J., Emerson, C.C., Stewart, P.L. and Kolios, M.C., 2019. Contrast enhanced ultrasound imaging by nature-inspired ultrastable echogenic nanobubbles. Nanoscale, 11(33), pp.15647-15658.

[15] Perera, R.H., Wu, H., Peiris, P., Hernandez, C., Burke, A., Zhang, H. and Exner, A.A., 2017. Improving performance of nanoscale ultrasound contrast agents using N, N-diethylacrylamide stabilization. Nanomedicine: Nanotechnology, Biology and Medicine, 13(1), pp.59-67.

[16] Feshitan, J.A., Chen, C.C., Kwan, J.J. and Borden, M.A., 2009. Microbubble size isolation by differential centrifugation. Journal of colloid and interface science, 329(2), pp.316-324.

[17] R.E. Caflish, M.J. Miksis, G.C. Papanicolaou, L. Ting, Effective equations for wave propagation in bubbly liquids, J. Fluid Mech. 153 (1985) 259–273.

[18] O. Louisnard, A simple model of ultrasound propagation in a cavitating liquid. Part I: Theory, nonlinear attenuation and traveling wave generation, Ultrason. Sonochem. 19 (2012) 56–65.

[19] Marmottant, P., Van Der Meer, S., Emmer, M., Versluis, M., De Jong, N., Hilgenfeldt, S. and Lohse, D., 2005. A model for large amplitude oscillations of coated bubbles accounting for buckling and rupture. The Journal of the Acoustical Society of America, 118(6), pp.3499-3505.

[20] Haghi, H., Sojahrood, A.J. and Kolios, M.C., 2019. Collective nonlinear behavior of interacting polydisperse microbubble clusters. Ultrasonics sonochemistry, 58, p.104708.

[21] Doinikov, A.A., Haac, J.F. and Dayton, P.A., 2009. Modeling of nonlinear viscous stress in encapsulating shells of lipid-coated contrast agent microbubbles. Ultrasonics, 49(2), pp.269-275.

[22] AJ Sojahrood, H Haghi, Q Li, TM Porter, R Karshafian, MC Kolios, (2019) Nonlinear energy loss in the oscillations of coated and uncoated bubbles: Role of thermal, radiation damping and encapsulating shell at various excitation pressures, arXiv preprint arXiv:1909.08793.